# Incremental Motor Skill Learning and Generalization from Human Dynamic Reactions based on Dynamic Movement Primitives and Fuzzy Logic System

Zhenyu Lu, *Member, IEEE,* Ning Wang, *Member, IEEE,* and Miao Li, Chenguang Yang, *Senior Member, IEEE*

*Abstract*—**Different from previous work on single skill learning from human demonstrations, an incremental motor skill learning, generalization and control method based on dynamic movement primitives (DMP) and broad learning system (BLS) is proposed for extracting both ordinary skills and instant reactive skills from demonstrations, the latter of which is usually generated to avoid a sudden danger (e.g., touching a hot cup). The method is completed in three steps. First, the ordinary skills are basically learned from demonstrations in normal cases by using DMP. Then the incremental learning idea of BLS is combined with DMP to achieve multi-stylistic reactive skill learning such that the forcing function of the ordinary skills will be reasonably extended into multiple stylistic functions by adding enhancement terms and updating weights of the radial basis function (RBF) kernels. Finally, electromyography (EMG) signals are collected from human muscles and processed to achieve stiffness factors. By using fuzzy logic system (FLS), the two kinds of skills learned are integrated and generalized in new cases such that not only start, end and scaling factors but also the environmental conditions, robot reactive strategies and impedance control factors will be generalized to lead to various reactions. To verify the effectiveness of the proposed method, an obstacle avoidance experiment that enables robots to approach destinations flexibly in various situations with barriers will be undertaken.**

*Index Terms*—**Learning from demonstration, Fuzzy logic system, Dynamic movement primitive, Broad learning, Impedance control**

## I. INTRODUCTION

LEARNING from demonstrations (LfD) provides a low-cost and effective way for robot programming and draws a lot of research attention in recent decades [1]. Dynamic movement primitives (DMP), proposed by Schaal [2], is a practical branch of LfD and firstly enables an artificial agent to act a complex human-like action in a versatile and creative manner [3]. As is mentioned in [3], DMP is full of advantages, such as simple and elegant formulation, convergence to a given target, flexiblity
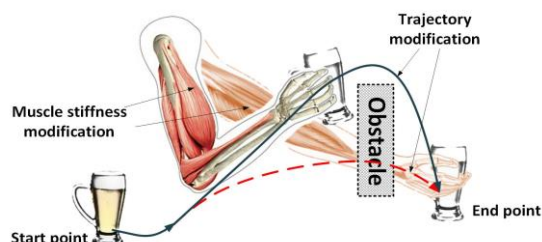


Fig.1 Illustration of human dynamic reactions

for complex behaviors, and capability of reacting to some external perturbations. DMP is then developed to many algorithms, such as orientation DMP, rotation matrix DMP, and is widely used for cooperative manipulation [4], [5], obstacle avoidance [6]-[13] and variable impedance control [14], [15].

As seen from previous research, most published DMP-related methods extracted skills from single or multiple demonstrations performed in the same task, which are named as **ordinary skills** in this paper. In the case exhibited in Fig.1, a person picks up a cup from the start position and takes it to the destination following the red path. When a human faces a sudden obstacle or danger, his or her muscles will make a nervous reaction to avoid conflict. This muscle shrink reaction, defined as the **reactive skill** in this paper, has seldom been discussed in previous robot skill learning research. This reactive skill has two characteristics:1 ) it is an additional skill, in that if there is no accident, it will not be activated, and the human will move as originally planned. If an accident occurs, the reactive skill will act to change the ordinary path.; 2) Different people react differently. Humans will follow their accustomed way of doing business. Therefore, this paper aims to propose a method for realizing both ordinary and characteristic reactive skills learning and generalization.

First, we will compare this study issue with related research topics on DMP-based obstacle avoidance and incremental skill

Zhenyu Lu, Ning Wang and Chenguang Yang are with the Bristol Robotics Laboratory, University of the West of England, BS16 1QY, United Kingdom. Miao Li is with the Institute of Technological Sciences, Wuhan University, Wuhan 430072, People's Republic of China.

learning. Obstacle avoidance is a typical application of DMP demonstrated by adding a potential field term to modify the original function to enable the generalized to satisfy the special constraints [6], [7]. Hoffmann et. al inspired by biological information and human behaviors to build an acceleration term calculated by position of obstacle and velocity of robots to realize static and moving obstacle avoidance [8]. Khansari-Zadeh et. al studied this issue by using dynamical systems (DSs) to ensure the impenetrability of multiple convex shaped obstacles [9]. Gam et. al proposed an adaptive DMP by adding a feedback term to the accelerating calculation of DMP for the instantaneous reactions. However, feedback term is a simplified proportional control law with a constant gain [10]. More recent research combined DMP with control methods for online path planning and control [11], [12], which is expected to develop to realize robots cooperation [16] or biped robot control [17]. For unknown obstacles, the above methods mostly choose to add an extra designed term to modify DMP function. But the solution for realizing obstacle avoidance is not unique and may be simultaneously affected by other constraints. So, the modified trajectory, after adding a force field term or a predesigned control diagram, may not be available in a way that humans would actually do.

To enable skills to be continually improved after adding new demonstrations, some researchers proposed integrating DMP and incremental learning method [1]. Kulić et. al, proposed an on-line, incremental learning of full body motion primitives. Both motion primitives and primitive sequencing are learned and integrated in a framework to enable robots to complete humanoid motions [18]. Lemme et. al, also studied this issue and built a movement primitive library (MPL) by using self-supervised bootstrapping. The MPL is then used to compose and decompose complex trajectories by sequencing primitives. New movement primitive will be learned to extend the MPL to realize incremental learning [19]. However, these DMPs are placed as nodes to be connected to generate complex actions but are not updated along with new added demonstrations. The recent research of Wang and Wu et. al proposed DMP plus method of inserting a bias term to the DMP implementation to let the original system to learn a new given task accurately [25], [26]. Compared with other DMP-based incremental learning methods, the work of Wang and Wu et. al realized primitive skill-level learning, not merely the task-level, that can enrich usability of the existing primitives to create complex actions effectively. Additionally, some research presented methods for learning and generalizing primitive skills based on DMP to realize multiple stylistic skills [18]-[24] and skill adaptation [22] or interactive behavior [23].

The above-mentioned studies are mostly about ordinary skill learning, and every subject is proposed with different usages and limitations, like DMP for obstacle avoidance cannot generalize humanoid style skills, and stylistic DMP can learn multiple types of skills but cannot address cases out of plan and realize skill adaptation to the changes of the environment. Incremental learning-based DMP keeps learning skills from new demos but can't generate stylistic skills to the new cases in [20], [21]. To our best knowledge, there is little research about the topic of stylistic incremental skill learning to acquire both ordinary and reactive skills to solve the task presented in Fig. 1. Additionally, the path points achieved by DMP can be utilized for multi-robot cooperation [16] or biped robot control [17] to realize obstacle avoidance and model-free motion tracking [12].

To address the above challenges, this paper presents an incremental motor skill learning, generalization and impedance control framework with following contributions:

1. Proposing a hierarchical skill learning diagram to realize both ordinary skill and reactive skill learning, such that the learned results can cover the ordinary operations as well as cases out of plan.

2. To realize stylistic reactive skill learning, the idea of broad learning system (BLS) and DMP are integrated to enable the forcing function of DMP (a nonlinear term introduced in eq. (3)) to keep updating by calculating stylistic factors, adding enhancement terms and updating weight terms. The acquired reactive skills are expected to be combined with the ordinary skills, learned by original DMP, to achieve an entire dynamic reaction.

3. To realize skill generalization with different conditions, a FLS-based stylistic skill generalization method is proposed. A fuzzifier is built to acquire a nonlinear reactive skill term with several fuzzy sets and rules about shapes, locations of the obstacle, human operational strategies and muscle stiffness to create suitable reactions for varying environmental conditions. Then the skills can be generalized by changing not only start, end, and scaling as normal but also strategies, control impedances and moving directions.

4. Based on the above contributions and our previous work of using the muscle stiffness for robot impedance control [14], [15], we proposed an adaptive impedance control based on the generalized outputs to realize the system stability with considerations of contact force estimation errors and robot uncertain dynamics.

The reminder of this paper is organized as follows: Section II introduces the model and properties of a robot system, as well as basic knowledge of DMP, BLS and FLS. Section III contains three parts to show the detailed work in contributions. Section IV concerns an experiment using robots to complete a picking-and-placing task to present human demonstration, skill learning, generalization in real applications. Section V gives a conclusion.

## II. RELATED WORK

### A. Modelling of robot

Considering the following robot arm dynamics described by a Lagrangian formulation:

$$M\ddot{q} + C(\dot{q},q)\dot{q} + G(q) + f(\dot{q}) = J(q)F_e + \tau, \quad (1)$$

where $q$ and $\dot{q}$ are n-dimensional vectors of robot joint position and velocity, $M$ is a $n \times n$ symmetric positive-definite robotic inertia matrix, $C(\dot{q},q)$ is a $n \times n$ matrix of Centripetal and Coriolis torque vector, $G(q)$ is the gradients of gravitational

potential energy, $f(\dot{q})$ is the external friction vector, $F_e$ is an environmental contact force, $J(q)$ is a Jacobian matrix and $\tau$ is the control torque to design. The system (1) has the following properties

**Property 1**. The matrix $\dot{M} - 2C(\dot{q}, q)$ is skew-symmetric.

**Property 2**. [27] Set $L$ as smallest achievable sampling period in digital implementation, and the sampling rate is usually faster than 30 times. For the model in (1), $F_e$ is considered as a hard nonlinearity satisfying $F_e^{(t)} \neq F_e^{(t-L)}$ as a discontinuous function, and $f(\dot{q})$ and $J(q)$ are continuous and soft nonlinearities estimated by time delay estimation (TDE) as $f(\dot{q})^{(t)} \cong f(\dot{q})^{(t-L)}$ and $J(q)^{(t)} \cong J(q)^{(t-L)}$.

**Property 3**. [28] Changes of contact forces within time interval $L$ are $\Delta F_e^{(t)} = F_e^{(t)} - F_e^{(t-L)}$ and limited by

$$\left| \Delta F_e^{(t)} \right| < \varepsilon . \tag{2}$$

where $\varepsilon$ is a constant and estimated by measurements in actual.

**Property 4**. : In any finite work space, $J(q)$ is nonsingular and bounded by $|J(q)| \leq \alpha$.

### B. Dynamic movement primitives

The DMP model for a task-space motion is presented as

$$\begin{cases} \tau \dot{v} = K(g - x) - Dv + (g - x_0) f(s), \\ \tau \dot{x} = v \end{cases} \tag{3}$$

where $K, D > 0$ are damping and stiffness coefficients in (3), and $\tau > 0$ is a scaling parameter for adjusting the duration of trajectory, and $f(s) = \theta^T \Psi(s)$ is a forcing function. where $\theta = [w_1, w_2, ..., w_n]^T$, $\Psi(s) = [\psi_1, \psi_2, ..., \psi_n]^T$ and $\psi_i$ is

$$\psi_i = \frac{\varphi_i(s)s}{\sum_{i=1}^{n} \varphi_i(s)}, \tag{4}$$

with Gaussian functions $\varphi_i(s) = \exp(-h_i(s - c_i)^2)$, where $c_i > 0$ and $h_i > 0$ are the centers and widths of radial basis functions. $f(s)$ depends on the phase variable $s$, which is calculated by a canonical system

$$\tau \dot{s} = -\gamma s, \quad \gamma > 0 . \tag{5}$$

### C. Broad learning system

BLS is proposed based on the random vector functional-link neural network (RVFLNN) and inherits the merit of effectively eliminating the drawback of the long training process [29]. BLS is a flat network, where the original inputs are transferred as "mapped features" in feature layer and the structure is expanded in a wide sense in the "enhancement nodes" (as Fig. 2 shown). In recent years, BLS has been used for robotic control [30], [31], and micro aerial vehicle control. In Fig. 2, $X$ is the input vector and $Y \in R^{N \times C}$ is the output variable of the network, where $N$ is the number of feature mapping and $C$ is the dimension of the
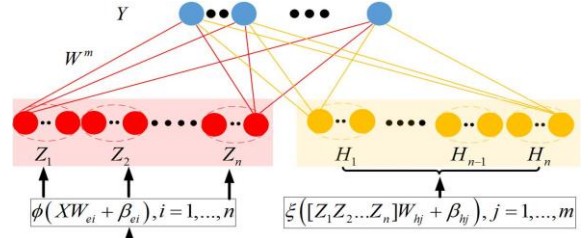

Fig.2 Illustration of BLS

network's output. In order to explore hidden features of input data, the feature mappings are expressed as

$$Z_i = \phi_i(X W_{ei} + \beta_{ei}), \quad i = 1, 2, ..., n , \tag{6}$$

where $\phi_i$ is a transformation function and $W_{ei}$ and $\beta_{ei}$ are randomly sampled from the distribution density. Setting $Z^n = [Z_1, Z_2, ..., Z_n]$, and the $j$th enhancement term $H_j$ of the functional link networks is generated by a linear function $\xi_j$, similar to $\phi_i$, as

$$H_j = \xi_j(Z^n W_{hj} + \beta_{hj}), j = 1, 2, ..., m . \tag{7}$$

where $W_{hj}$ and $\beta_{hj}$ are randomly generated sampling data from distribution density. Then linked network is expended by

$$\begin{aligned} Y &= \left[ Z_1, ..., Z_n \left| \xi(Z^n W_{e1} + \beta_{e1}), ..., \xi(Z^n W_{em} + \beta_{em}) \right. \right] W \\ &= \left[ Z_1, ..., Z_n \left| H_1, ..., H_m \right. \right] W \\ &= \left[ Z^n \left| H^m \right. \right] W \\ &= A^{n+m} W \end{aligned} \tag{8}$$

where $X^N = [X | x]$ represents the matrix $X$ is extended in row by $x$ to achieve a new matrix $X^N$.

In (8), matrix $W$ represents weights for the extended feature matrix $[F^n | H^m]$ and can be calculated by the pseudo-inverse calculation $W = [F^n | H^m]^+ Y$. After adding new feature terms $H^m$, $W$ will be updated based on the calculation of the pattern matrix $[F^n | H^m]^+$. Setting $A^{n+1} = [A^n | a]$, where $a$ is a new enhancement matrix, then the matrix $W^{n+1}$ is updated by

$$W^{n+1} = \begin{bmatrix} W^n - db^T Y_n \\ b^T Y_n \end{bmatrix}, \tag{9}$$

where $d = (A^n)^+ a$, $b^T = \begin{cases} c^+ & \text{if } c \neq 0 \\ (1 + d^T d)^{-1} d^T (A^n)^+ & \text{if } c = 0 \end{cases}$,

$c = a - A^n d$.

### D. Fuzzy approximation

Fuzzy approximation has been used for controlling robot [32], exoskeleton [33], pneumatic artificial muscle (PAM) [34] and

mobile wheeled inverted pendulum[35]. Here, we consider an $n_i$ inputs, single-output fuzzy logic system with the product-inference rules, singleton fuzzifier, defuzzifier, and Gaussian membership function given by $n_j$ fuzzy IF–THEN rules:

$$R^{(j)}: \text{IF } x_1 \text{ is } A_1^j \text{ and ... and } x_{ni} \text{ is } A_{ni}^j \text{ THEN } y \text{ is } B^j, \quad (10)$$

$$j = 1,..,n_j$$

where $R^{(j)}$ denotes the $jth$ rule , $(x_1, x_2,..., x_{n_j})^T \in U$ and $y \in R$ are linguistic variables associated with FLS inputs and output respectively. $A_i^j$ and $B^j$ are fuzzy sets in $U$ and $R$. Then the FLS performs a nonlinear mapping from $U$ to $R$. We use the strategy of singleton defuzzification, and the output of product inference and center-average defuzzification, the FLS is

$$y(x) = \frac{\sum_{j=1}^m y_j \left( \prod_{i=1}^n \mu_{A_i^j}(x_i) \right)}{\sum_{j=1}^m \left( \prod_{i=1}^n \mu_{A_i^j}(x_i) \right)}, \quad (11)$$

where $x = [x_1, x_2,..., x_m]^T$ and $\mu_{A_i^j}(x_i)$ represents membership functions of the linguistic variable $x_i$.

### III. BLS-BASED SKILL LEARNING, GENERALIZATION AND CONTROL

In this section, we present a robot incremental skill learning and generalization, and the related impedance control framework, which consists of four stages colored with different backgrounds in Fig.3.
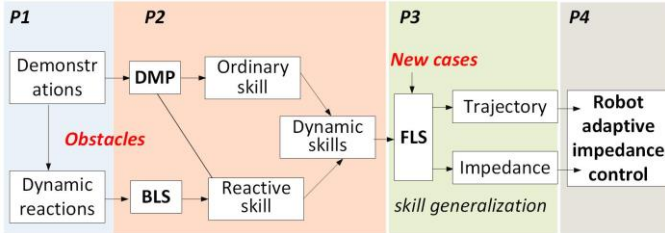


Fig.3 Composition for dynamic stylistic skill learning and control framework

First, human operators create demonstrations in the known environment and dynamic reactions for the suddenly appeared obstacles (P1). For different obstacles, the demonstrating conditions e.g., human decisions, reactive motions and muscle stiffness are recorded. P2 is about skill learning. The ordinary skills and stylistic reactive skills are separately learned from normal actions and sudden reactions that are collectively called **dynamic skills** and introduced in detail in Subsection A. As the reactive skills are determined by objective conditions, such as the size and location of obstacles as well as the decision of the actuator unit (human/robot), we describe these factors by fuzzy sets and use FLS to realize skill generalization in space and time with more interactions with the environment (P3, in Subsection B). For a new task, trajectories and impedance factors are separately generalized and used for robot impedance control (P4, in Subsection C).

#### A. BLS-based incremental stylistic skill learning

First, we assume that the reactive motions are generated by new accidents. But they don't change the start and end points. Only the interval path points are changed between the start and destination. Then the new trajectory under the influence of obstacles with a new forcing term $f^N(s)$ is

$$\begin{cases} \tau \dot{v} = K(g-x) - Dv + (g-x_0)f^N(s) \\ \tau \dot{x} = v \end{cases}. \quad (12)$$

The term $f^N(s)$ is designed following the 'broaden' idea of BLS that part of Gaussian functions are chosen from the original $f(s)$, and some enhancement terms $\eta_j(s), j = 1,2,...,m$ will be added into $f^N(s)$ to improve the nonlinear fitting effect to a new trajectory based on $\Phi(s) = [\varphi_1(s),...,\varphi_n(s)]$, where $\varphi_i(s)$ is the Gaussian function shown in (4):

$$\eta_j(s) \equiv \zeta_j (\Phi(s)W_j + \beta_j), \quad (13)$$

where $\zeta_j$ is a transformation function similar to $\xi$ in (7), and $W_j$ and $\beta_j$ are randomly generated weights.

The original $\varphi_j(s)$ and new added $\eta_j(s)$ will be normalized to generate new state terms $\lambda_k, k = 1,...,m+n$

$$\lambda_k = \frac{q_k(s)\varphi_k(s) + (1-q_k(s))\eta_{k-n}(s)}{\sum_{i=1}^n \varphi_i(s) + \sum_{j=1}^m \eta_j(s)} s, \quad (14)$$

satisfying $\sum_{k=1}^{m+n} \lambda_k = s$, where $\begin{cases} q_k(s) = 1, & k \in [1,n] \\ q_k(s) = 0, & k \in [n+1,n+m] \end{cases}$.

Setting $\Gamma \sum_{i=1}^n \varphi_i(s) = \sum_{i=1}^n \varphi_i(s) + \sum_{j=1}^m \eta_j(s)$, we can get $\sum_{i=1}^n \varphi_i(s) + \sum_{j=1}^m \eta_j(s) = \frac{\Gamma}{\Gamma-1} \sum_{j=1}^m \eta_j(s)$. It is obvious that if terms $\varphi_i(s)$ and $\eta_j(s)$ are fixed, then $\Gamma$ has a confirmed value. Then $\lambda_k$ is expressed by $\psi_i$ and $\eta_j(s)$ as:

$$\begin{aligned} \lambda_k &= \frac{q_k(s)\varphi_k(s)s}{\sum_{i=1}^n \varphi_i(s) + \sum_{j=1}^m \eta_j(s)} + \frac{(1-q_k(s))\eta_{k-n}(s)s}{\sum_{i=1}^n \varphi_i(s) + \sum_{j=1}^m \eta_j(s)} \\ &= \frac{q_k(s)\varphi_k(s)s}{\Gamma \sum_{i=1}^n \varphi_i(s)} + \frac{(\Gamma-1)(1-q_k(s))\eta_{k-n}(s)s}{\Gamma \sum_{j=1}^m \eta_j(s)} \\ &= \frac{q_k(s)\psi_k(s)}{\Gamma} + \frac{(\Gamma-1)(1-q_k(s))\eta_{k-n}(s)s}{\Gamma \sum_{j=1}^m \eta_j(s)} \end{aligned} \quad (15)$$

where $\eta_{k-n}(s)=0$, if $k-n<0$. Term $\lambda_k$ corresponds with a new linear vector $\theta_{n+m}^N$, which is expressed as $\theta_{n+m}^N = [w_1, w_2,..., w_n | u_1, u_2,..., u_m]^T = [\theta | \theta^U]^T$, where $u_j, j = 1,...,m$ are additional weights.

Set $\gamma_j(s) = \dfrac{\eta_j(s)s}{\sum_{j=1}^m \eta_j(s)}$ and $\Upsilon(s) = [\gamma_1(s),...,\gamma_m(s)]$, then

$$
\begin{aligned}
\Xi(s) &= \left[\lambda_1, \lambda_2,...,\lambda_{n+m}\right]^T \\
&= \left[\psi_1(s)/\Gamma,...,\psi_n(s)/\Gamma \middle| (\Gamma-1)\gamma_1(s)/\Gamma,...,\right. \\
&\quad \left. (\Gamma-1)\gamma_m(s)/\Gamma\right]^T \\
&= \left[\Psi(s)/\Gamma \middle| (1-1/\Gamma)\Upsilon(s)\right]^T
\end{aligned} \quad (16)
$$

Then the new forcing function $f^N(s)$ can be expressed as

$$
\begin{aligned}
f^N(s) &= \left(\theta_{n+m}^N\right)^T \Xi(s) \\
&= (1/\Gamma)\theta^T \Psi(s) + (1-1/\Gamma)\left(\theta^U\right)^T \Upsilon(s) \\
&= (1/\Gamma)f(s) + (1-1/\Gamma)f^U(s) \\
&= f(s) + (1/\Gamma-1)\left(f(s) - f^U(s)\right)
\end{aligned} \quad (17)
$$

where $f^U(s) = \left(\theta^U\right)^T \Upsilon(s)$.

**Remark 1**: The combination of BLS and DMP is realized by adding enhancement terms $\eta_j(s), j=1,...,m$. Then the weights $\theta_{n+m}^N$ and state vector $\Xi(s)$ are extended from $\theta$ and $\Psi(s)$. By adding and normalizing more enhancement nodes, $f^N(s)$ will be improved to generate more complex trajectories.

Compared with (3), the error term

$$
\begin{aligned}
\Delta f(s) &= f^N(s) - f(s) \\
&= (1/\Gamma-1)\left(f(s) - f^U(s)\right)
\end{aligned} \quad (18)
$$

can be seen as a reactive skill adding to the ordinary one.

Term $\Delta f(s)$ can be expressed in a linear form as

$$
\Delta f(s) = \theta_{n+m}^N \Xi^A(s), \quad (19)
$$

where $\Xi^A(s) = \left[(1/\Gamma-1)\Psi(s) \middle| (1-1/\Gamma)\Upsilon(s)\right]^T$.

**Remark 2**: The reactive skill term $\Delta f(s)$ in (19) is expressed in a similar form as $f(s)$. After adding a new term $\eta_j(s)$, $\theta_{n+m}^N$ and $\Xi^A(s)$ both will be extended and $\Gamma$ will be changed as well. According to the theory of BLS, $\Delta f(s)$ can approach to any nonlinear trajectory with the increase of enhancement nodes. Vector $\Xi^A(s)$ has two parts: one is $(1/\Gamma-1)\Psi(s)$ representing changes of $\Psi(s)$ after adding new enhancement nodes and the other is $(1-1/\Gamma)\Upsilon(s)$ to prolong the state vector.

In the DMP, the target value of $f(s)$ is calculated by

$$
\min \sum_{j=1}^n \left\| f_j^{Tar}(s) - f(s) \right\|, \quad (20)
$$

where

$$
f_j^{Tar}(s) = \left(\tau\dot{v}_j - K(g-x_j) - Dv_j\right)/(g-x_0), \quad (21)
$$

and weights $\theta$ are learned by supervised learning algorithms such as k-means clustering algorithm to minimize (20).

The target value of $f_j^N(s)^{Tar}$ is derived from (12) as

$$
f_j^N(s)^{Tar} = \left(\tau\dot{v}_j^N - K(g-x_j^N) - Dv_j^N\right)/(g-x_0). \quad (22)
$$

where $x_j^N$ and $v_j^N$ represent the position and velocity of the $j$th reactive trajectory. Then the desired value of $\Delta f(s)$ is acquired based on the calculation of $f(s)$ as

$$
\begin{aligned}
\Delta f_j(s)^{Tar} &= f_j^N(s)^{Tar} - f(s) \\
&= \frac{\left(\tau(\dot{v}_j^N - \dot{v}) - D(v_j^N - v) + K(x_j^N - x)\right)}{g-x_0},
\end{aligned} \quad (23)
$$

and then the reactive skill can be calculated by minimizing

$$
\min \sum_{j=1}^m \left\| \Delta f_j^{Tar}(s) - \Delta f(s) \right\|. \quad (24)
$$

Using (20) and (24), the ordinary skill and reactive skill will be acquired gradually. However, (24) is used to get only one group of $\theta_{n+m}^N$ to achieve one kind of reactive skill. To acquire multi-stylistic reactive skills, we propose the following method based on the previous equations. First, we assume that multiple reactive skills $\Delta f^k(s), k=1,...,K$ are derived from the common ordinary skill calculated by $f(s)$ and these reactive skills are learned based on the common state vector $\Xi^A(s)$ in (19) as

$$
\Delta f^k(s) = \left(\theta_{n+m}^N\right)^k \Xi^A(s), \quad (25)
$$

and the weights $\theta_{n+m}^N$ will be regressed into different values. Furthermore, we define a stylistic coefficient $\lambda_k, k=1,2,...,K$ to normalize $\theta_{n+m}^N$ and (25) is expressed as

$$
\Delta f^k(s) = \lambda_k \theta_{n+m}^N \Xi^A(s) = \lambda_k \Delta f^B(s). \quad (26)
$$

In [18], the authors improved DMP by proposing a stylistic-attractor landscapes instead of the forcing function. The weights for different styles are calculated based on the SVD calculation for target matrices. We also use SVD division for calculating stylistic factor $\lambda_j$ based on the matrix $\Delta F(s)^{Tar} = \left[\Delta f_1(s)^{Tar},\right.$ $\left.\Delta f_2(s)^{Tar},...,\Delta f_K(s)^{Tar}\right]$ as

$$
\Delta F(s)^{Tar} = U\Sigma V^T \approx M\left(\Delta F^B(s)\right)^{Tar}, \quad (27)
$$

and $\lambda_j$ is the $j$th item of $M = [\lambda_1, \lambda_2,...,\lambda_K]$ and $\Delta F^B(s)^{Tar} = \left[\left(\Delta f_1^B(s)\right)^{Tar}, \left(\Delta f_2^B(s)\right)^{Tar},...,\left(\Delta f_K^B(s)\right)^{Tar}\right]$. Then the weights $\theta_{n+m}^N$ are calculated by

$$\min \sum_{k=1}^{K} \left\| \left( \Delta f_k^B (s) \right)^{Tar} - \Delta f^B (s) \right\|. \tag{28}$$

The calculation procedure for the ordinary skill and reactive skills learning is realized by the following three steps:

1) **Step 1**: Using normal demonstrations and (3) and (5) to learn a general skill to approach to the target function (20). The weights $\theta$, state vector $\Psi(s)$ and forcing function $f(s)$ will be achieved after calculation.

2) **Step 2**: Human will make reactions for different situations and the key influence factors leading to the reactions will be recorded along with reactions. By using (22) and (23), $\Delta f_k (s)^{Tar}, k = 1, ..., K$ are achieved and further transformed to $\left( \Delta f_k^B (s) \right)^{Tar}$ based on the SVD division.

3) **Step 3**: Using weights $\theta$ and state vector $\Psi(s)$ acquired in **step 1** and equations (13) to (19), we can initialize weights $\theta_{n+m}^N$ and $\Xi^A(s)$ first and then use (24) to optimize $\theta_{n+m}^N$ to achieve reactive skills. The weights $\theta_{n+m}^N$ will be prolonged after adding new enhancement nodes. For multi-stylistic reactive skill learning, we will choose (26) to replace (19) and use (28) for optimization.

*B. FLS-based skill generalization*

DMP can realize skill generalization by changing start, end and scaling factor, but the generalized results are similar to the demonstrated ones. Even if we can use the method in Subsection A to get some reactive skills to change the ordinary skill in some extend, the results still can't cover all the cases that have never arisen before. By using demonstrating conditions recorded in **Step 2** and stylistic skills in **Step 3**, we build input fuzzy sets that have potential influences to the trajectories and muscle actions e.g., shapes of the obstacle, distance to the obstacle, and user's manipulating strategies, and IF–THEN rules to achieve reactive skills. For example , we set the distance from the start to the obstacle as $t_1$, the height of the obstacle as $t_2$, human moving direction as $t_3$, and the final reactive skills as output $o$. Then the $n_j$ IF–THEN rules are described as:

$R^{(1)}$:  IF $t_1$ is far and $t_2$ is tall and $t_3$ is left THEN $o$ is $\Delta f^1(s)$ ;

$R^{(2)}$ :  IF $t_1$ is close and $t_2$ is tall and $t_3$ is right THEN $o$ is $\Delta f^2(s)$ ;...

$R^{(n_j)}$ :  IF $t_1$ is close and $t_2$ is short and $t_3$ is right THEN $o$ is $\Delta f^{n_j}(s)$ ;

$$\tag{29}$$

We select Gaussian fuzzy membership functions in (30), $c_{ij}$ and $\sigma_{ij}$ represent the center and width of the *ith* fuzzy set $A_i^j$

$$\mu_{A_i^j} (x_i) = \exp \left[ -\frac{(x_i - c_{ij})^2}{\sigma_{ij}^2} \right]. \tag{30}$$

By using (11), the defuzzified reactive skill $\Delta f^F (s)$ are calculated by

$$\Delta f^F (s) = \frac{\sum_{j=1}^{n_j} \Delta f^j(s) \left( \prod_{i=1}^{n} \mu_{A_i^j} (x_i) \right)}{\sum_{j=1}^{n_j} \left( \prod_{i=1}^{n} \mu_{A_i^j} (x_i) \right)}$$
$$= \frac{\sum_{j=1}^{n_j} \lambda_j \theta_{n+m(j)}^N \Xi^A(s) \left( \prod_{i=1}^{n} \mu_{A_i^j} (x_i) \right)}{\sum_{j=1}^{n_j} \left( \prod_{i=1}^{n} \mu_{A_i^j} (x_i) \right)}. \tag{31}$$

**Remark 3**: As it is proven that FLS can uniformly approximate to any given continuous function over a compact set to any degree of accuracy. Eq. (31) can also be expressed as

$$\Delta f^F (s) = \frac{\sum_{j=1}^{m} \lambda_j \theta_{n+m(j)}^N \left( \prod_{i=1}^{n} \mu_{A_i^j} (x_i) \right)}{\sum_{j=1}^{m} \left( \prod_{i=1}^{n} \mu_{A_i^j} (x_i) \right)} \Xi^A(s) , \tag{32}$$

which can be seen as a nonlinear composition of $\theta_{n+m(j)}^N$ in (19) based on the same vector $\Xi^A(s)$ to generalize modified stylistic reaction skills. Thus, the reactive skills (31) can approximate to any reactions within the designed ranges.

The main problem occurred in the fuzzy skill generalization process is scope changes of the fuzzy sets. Because the fuzzy rules generated in the demonstrations may not fit to new tasks, such as for a 10 cm trajectory, 8 cm is a long distance, but for a 100 cm trajectory, it is a short distance. Thus the fuzzy sets and IF-THEN rules should be changed along with the ordinary skills generalization. Define the start and end in a new task as $G$ and $X_0$, sampling time interval as $T$ and trajectory position as $X$, using the learned function $f(s)$ in (3) , the skill generalizations satisfy

$$\begin{cases} T\dot{V} = K(G - X) - DV + (G - X_0) f(s) \\ T\dot{X} = \dot{V} \end{cases}. \tag{33}$$

Factors $c_{ij}$ and $\sigma_{ij}$ in (30) are reset as $C_{ij}$ and $\Delta_{ij}$ following the new generated trajectory point $X_i$ as

$$\mu_{A_i^j} (X_i) = \exp \left[ -\frac{(X_i - C_{ij})^2}{\Delta_{ij}^2} \right], X_i \in \left[ \underline{X}_i, \bar{X}_i \right]. \tag{34}$$

As $c_{ij}$ and $\sigma_{ij}$ in (30) are chosen based on human experience, the factors $C_{ij}$ and $\Delta_{ij}$ in (34) also rely on humans' selections. They can keep the same values as in (30), enlarge or decrease the values for several times for $c_{ij}$ and $\sigma_{ij}$ to enable fuzzy sets to cover the scope of whole task space.  Then the defuzzified reactive skills in (31) is revised as :

$$\Delta f^F (s) = \frac{\sum_{j=1}^{m} \lambda_j \theta_{n+m(j)}^N \Xi^A(s) \left( \prod_{i=1}^{n} \mu_{A_i^j} (X_i) \right)}{\sum_{j=1}^{m} \left( \prod_{i=1}^{n} \mu_{A_i^j} (X_i) \right)} \tag{35}$$

Then the final generalized dynamic skill is expressed as

$$\begin{cases} T\dot{V} = K(G-X) - DV + (G-X_0)(f(s) + \Delta f^F(s)) \\ T\dot{X} = V \end{cases}. \quad (36)$$

**Remark 4**: In our previous work [14], [15], humanlike variable impedance skills are abstracted from EMG signals for robot control. However, the values of impedance cannot be enlarged or reduced freely in a similar way to the trajectories due to the physiological limitations. Some IF conditions are determined by exact space metrics like the height or position of the obstacle and can be requantized, while others depend on demonstrators' habits and minds, like turning directions or nervous tensions, which are expected to be held as the same IF conditions as in demonstrations.

*C. Variable impedance control*

Some recent studies of EMG signals recognition are used for exoskeleton [36] and myoelectric hand control [37]. To enable robots to realize human-like control effect, some studies about skills learning used EMG signals for updating factors of DMP and realizing DMP-based variable impedance control. In our previous research [14], [15], the impedance is generalized and used for enduring heavier object in the vertical direction, While in [38], the "variable impedance behavior in robots is the active safety due to the soft 'giving in' for both robots and the environment". As the experimental results shown in the next section, when the manipulator end approaches an obstacle, the stiffness of human handling arm will increase to avoid conflict. Here, we set a controlling factor $K_{imp}$ that has a linear relation to muscle stiffness $X^{stf}$ as

$$K_{imp} = k_s X^{stf}, \quad (37)$$

where $k_s$ is a constant factor. Meanwhile, some manipulators don't provide force sensors and $f(\dot{q})$ in (1) is hard to be modelized accurately. For dynamics errors and unknown force information, we used neural networks (NN) for force sensorless admittance control previously [39], [40]. Following property 2, we use time-delayed estimation (TDE) for compensating these error terms in this paper. Define $q^d$ as the desired value of $q$, $e = q^d - q$, $\dot{e} = \dot{q}^d - \dot{q}$, and $r = \dot{e} + ke$, where $k$ is a constant and $\tau_e = f(\dot{q}) - JF_e$, then the controller is designed as

$$\tau = M(\ddot{q}^d + k\dot{e}) + C(\dot{q}^d + ke) + G(q) - \tau_e, \quad (38)$$

where $J$ represents a Jacobian matrix, and $\tau_e$ is a control term that is deduced by the delayed signals as

$$\begin{aligned} \tau_e &= \tau_e^{(t-L)} + K_{imp}r \\ &= M\ddot{q}^{(t-L)} + C\dot{q}^{(t-L)} + G(q)^{(t-L)} - \tau^{(t-L)} + K_{imp}r \end{aligned}, (39)$$

where $K_{imp}$ is impedance-related positive factor that is expressed as

$$K_{imp} = \max(k_s X^{stf}, sign(r)\Gamma \varepsilon r^{-1}), \quad (40)$$

where $\Gamma \gg \alpha$ is a large enough factor. Eq. (37) is improved by considering the estimation errors to achieve (40). Due to the

dynamics modeling and measuring errors, selecting a unsuitable constant $k_s$ may cause system instability. The impedance factor in (40) is designed to realize human-like muscle stiffness changes as well as to ensure system stability, which is proved by the following Lyaponov function:

$$V = r^T M r. \quad (41)$$

Taking (38) into (1) and using **Property 3**, we have

$$M\dot{r} + (C + K_{imp})r = \tau_e - \tau_e^{(t-L)} = J(F_e - F_e^{(t-L)}). \quad (42)$$

Taking (42) into the time derivative of $V$, we have

$$\begin{aligned} \dot{V} &= 2\dot{r}^T M r + r^T \dot{M} r \\ &= 2J(F_e - F_e^{(t-L)})r + r^T \dot{M}r - 2r^T Cr - 2r^T K_{imp}r \\ &= 2J\Delta F_e r - 2r^T K_{imp}r \\ &\le 2\alpha\varepsilon r - 2r^T K_{imp}r \end{aligned} \quad (43)$$

Using (40), we have $\dfrac{sign(r)K_{imp}r}{\Gamma} \ge \varepsilon$, then (43) can be simplified as

$$\dot{V} \le 2\left(\frac{\alpha}{\Gamma} - 1\right)r^T K_{imp}r < 0. \quad (44)$$

## IV. EXPERIMENTS

The experimental platform in Fig.4 consists of a Touch Omni joystick, a 3D-print finger handle, a 21cm*13cm operational board, an 3D-print obstacle and a MYO armband for measuring EMG signals of operator's limb. The tool is fixed at the tip of the Touch joystick and can be replaced by a gripper driven by a servo motor. The height of obstacle can be modified by adding or reducing several 2cm*2cm*2cm cubes. Using the 3D-print handle, the operator can put a finger into a fixing hole and drag the end of the joystick to move from start (2,3,0) to the end (20,9,0), and the Touch joystick will record the joints and end positions. At the same time, human muscle EMG signals are also recorded. To acquire different demonstrations from start to the end, we change operational situations (presented in Table 1) by adding obstacles with different heights and placing them at different positions. The demonstrator will choose three directions (right, middle and left) to cross obstacles and the various reactions will be recorded. Fig.5 shows a demonstration with a high obstacle placed at the long-distance position (13,5).
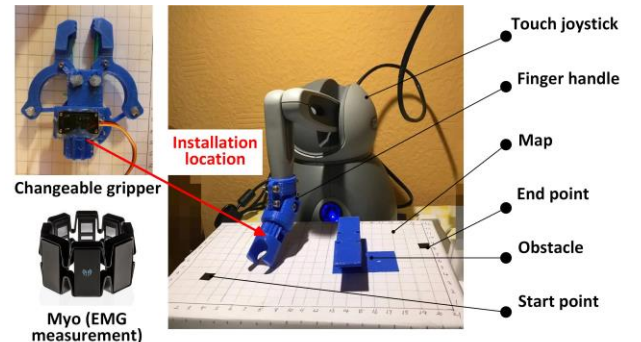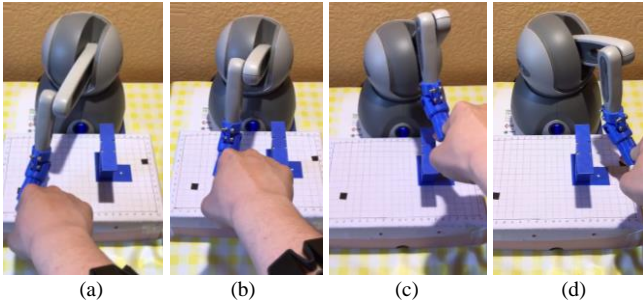


Fig. 4. Experimental platform

Fig.5 Process of demonstrations (High obstacle placed at the far location)

TABLE I
FACTORS AND EXPERIMENTAL CONDITIONS

| Factors | Experimental conditions |
|---|---|
| Distance to obstacle | Short distance |
| | Long distance |
| Height of obstacle | Tall (8cm) |
| | Low (2cm) |
| Direction | Left |
| | Forward |
| | Right |

### A. DMP/BLS-based skill learning

Following the experimental procedure (**Step 1** to **Step 3**) shown in Section III.A, we firstly demonstrate and record the ordinary actions and stiffness changes (grey dash lines in Fig. 6(a) and Fig. 6(b)). By using (3) and (5), the general skills are abstracted from the demonstrations (red lines in Fig. 6(a) and Fig. 6(b)) as the basis and benchmark case for the reactive skills
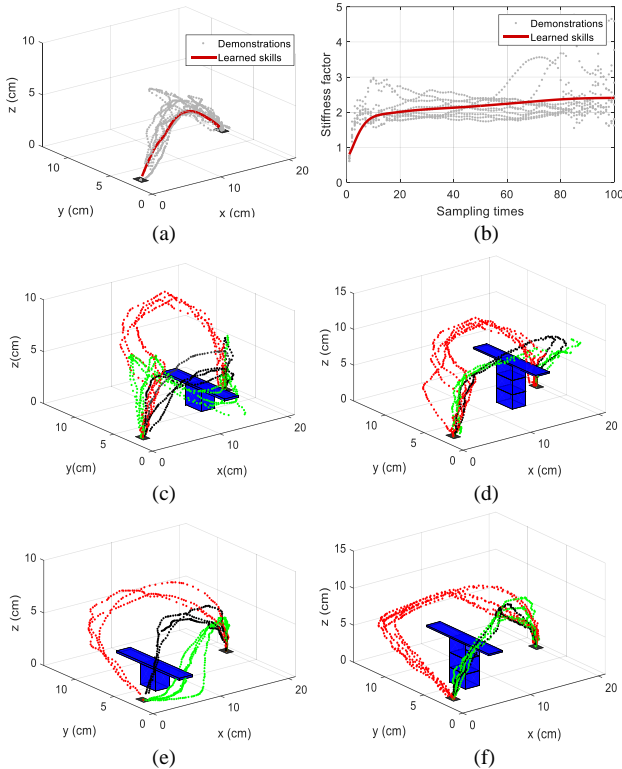


Fig.6 Skill demonstrations and ordinary skill learning (a) ordinary skill learning of trajectories; (b) ordinary skill learning of muscle stiffness; (c) trajectories with a low obstacle at the far location; (d) trajectories with a high obstacle at the far location; (e) trajectories with a low obstacle at the close location; (f) trajectories with a high obstacle at the close location
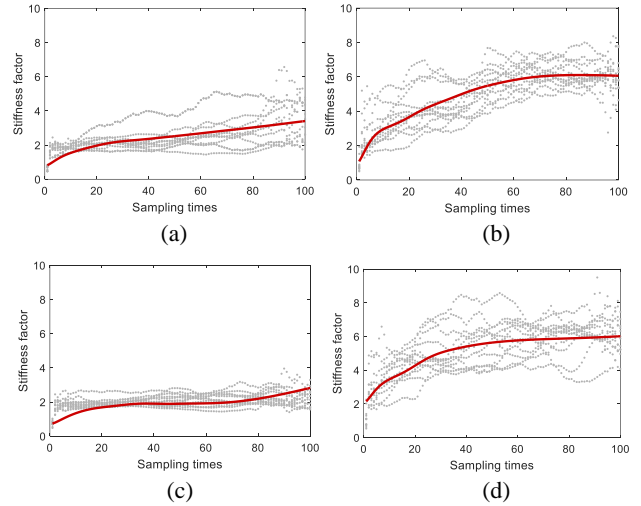


Fig.7 Stiffness changes for different cases (a) results with a low obstacle at the far location (b) Skill results with a high obstacle at the far location (c) results with a low obstacle at the close location (d) Skill results with a high obstacle at the close location
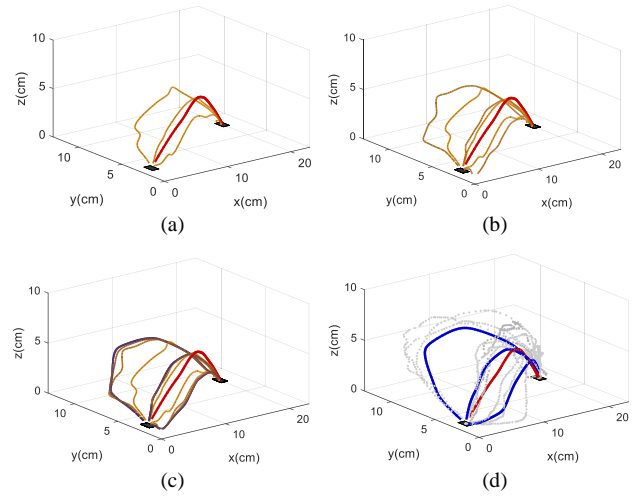


Fig.8 Reactive trajectory learning process (a) Results of adding one group of enhancement node; (b) Results of adding two groups of enhancement nodes; (c) Results of adding five groups of enhancement nodes; (d) Final learned results and classified demonstrations

learning. The trajectories measured in the special conditions in Table 1 are presented from Fig. 6(c) to Fig. 6(f). Three colored line bundles show trajectories with different moving directions. We can get a rough conclusion that for the lower obstacle, the trajectories are easy to be distinguished in different directions but for a higher obstacle, the forward and right motions override with each other and are hard to be divided due to the mechanical design of 3D tool and limited working space of joystick.

Fig. 7 shows impedance changes for different reactions. We find that the impedance is mainly determined by the shape and location of the obstacle and does not has much corresponding with the moving directions on the same level. Thus, we present impedance changes in four figures divided by different obstacle heights and locations. The compare of (a) and (b) shows that the impedance increases with the height of the obstacle by changing from 1 block to 3 blocks. The compare of (a) and (c), and (b) and (d) with the same height but different object locations show the tiny changes affected by the increasing speed of impedance such that when the obstacle is moved toward the start, operators

will enlarge impedance ahead for crossing over obstacles. But the final reaching values are similar.

Following **Step 2** and **Step 3** in Section III.A, the reactive motions are derived from the ordinary one in Fig.6 by adding enhancement nodes and extending members of weights and the common state vector $\Xi^A(s)$ in (25) . Fig. 8 (a) to (c) present the learning process after adding 1, 2 and 5 enhancement terns for the task with a lower obstacle and short-distance location. With the increase of enhancement nodes and updating of weights, the trajectories are expended in three directions from the ordinary to approach to the classified demonstrated reactions gradually. Fig.8 (d) shows the final learned results as well as demonstrated reactions. The learned reactive skills can represent the classified trajectory groups with minor errors.

### B. FLS-based stylistic skill generalization

The learned skills are generalized through several steps. First, after knowing a new start, end and scaling factor, the ordinary trajectory is generalized by using DMP. In Fig. 9(a), we change the start to (4,6,0) and end point to (18,4,0). The new ordinary trajectory is colored in blue, compared with the old one colored in red. Second, we place a medium-height obstacle (4cm) at (10,5,0). Because the new trajectory will be generated on the same map, the IF-THEN rules are choosing as same as in the demonstrations. Considering the influence of the environment, we generalize the skill in three typical directions and the results are shown in Fig. 9(b). Compared to the cases with lower and higher obstacles, the overlaps of forward and right trajectories stand at the medium level. Additionally, the moving directions are determined by operator's strategies not by angles, thus we choose dimensionless standards to express the transitional state between the right and left trajectories and the centers of fuzzy sets are 0, 0.8, and 1. Finally, using (35), the movements with different directions are generalized as grey lines in Fig.9 (c) and we choose a left-forward direction as the final trajectory as the red line shown in Fig. 9(c). As it is mentioned in **Remark 4**, the stiffness has a close relationship with the obstacle's height and



(a)          (b)          (c)

(d)          (e)          (f)

Fig.10 Manipulation process by using a gripper (a) grasp an object; (b)~(f) object moving process

positions, thus we choose the average value of stiffness in lower and higher cases as start and end for impedance generalization. The final stiffness generalization results are shown in fig. 9 (d).

### C. Adaptive impedance control

To enable the joystick to work as an actuator, we choose the kinematic and dynamics estimation method introduced in [41]. The factors in (40) are set as $k_s = 10$ , $\varepsilon = 1$ , $\Gamma = 100$ and the experiment process from closing gripper to picking and placing the object to the destination are shown in Fig. 10, and the upper joint torques varying with time are shown in Fig. 11 (a) to (c). The adaptive impedance ensures system stability and tracking performance of the gripper to the trajectory generalized by FLS (Fig.11(d)).

The main difference of the proposed method to the previous methods is dividing skills into an ordinary skill and a reactive skill. The ordinary skill is learned ahead, and reactive skills are incrementally learned based on the results of the ordinary skill.
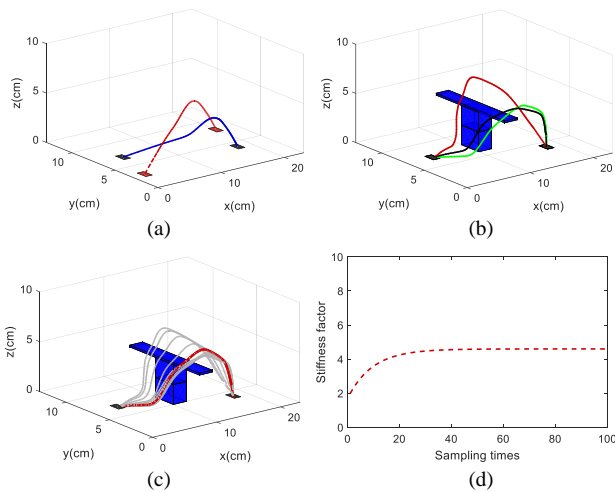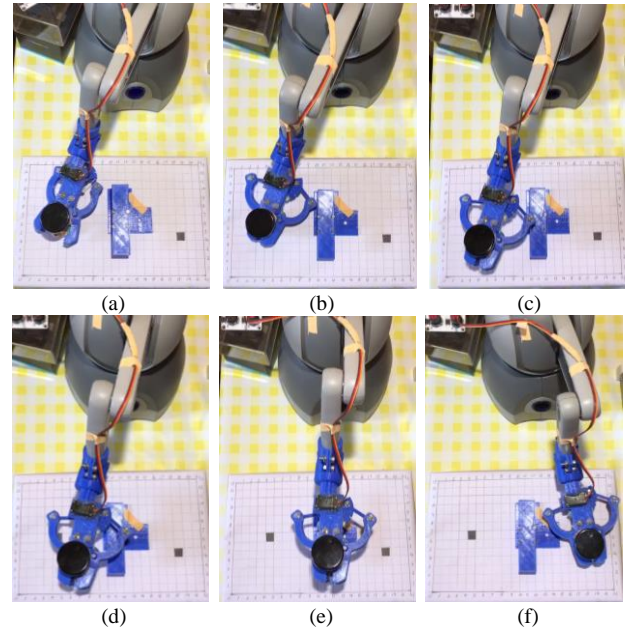


(a)          (b)

(c)          (d)

Fig.9 FLS-based skill generalization (a) ordinary skill generalization with new start and end points; (b) skill generalization with environmental factors (height and location of the obstacle); (c) skill generalization with environmental factors and operational strategies (moving directions); (d) generalization of muscle stiffness.
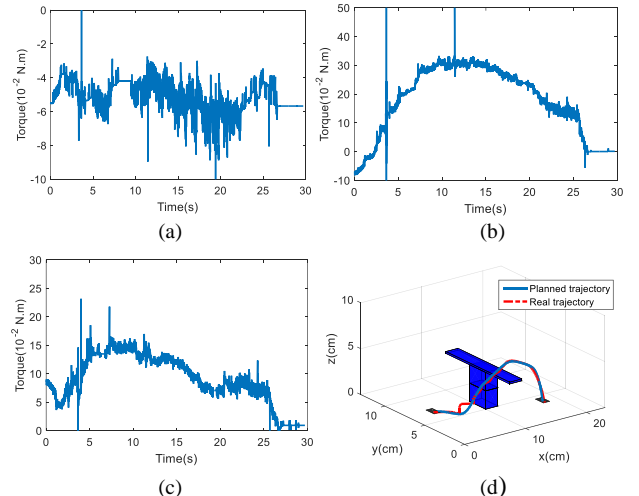


(a)          (b)

(c)          (d)

Fig.11 Joint torques and planned and real trajectory (a)-(c) joint torque; (d) trajectories comparation

Thus, both two kinds of skills are kept and can be generalized separately and cooperatively. FLS method extends dimensions for skill generalization, not only in space and time but also with objective conditions such as environmental influences, human strategies and muscle stiffness by building multiple fuzzy sets.

## V. CONCLUSION

In this paper, we proposed an incremental skill learning and generalization method based on dynamic movement primitive, fuzzy logic and broad learning system and used the generalized stiffness for robotic impedance control. Different from previous skill learning methods from demonstrations, the method learns from human ordinary actions and reactions to sudden incidents comprehensively. Thus, the proposed method can realize skill generalization not only in space and time but also considering the environmental changes, muscle stiffness and decisions. The technical effectiveness is verified through an experiment that an object is picked by a desk robot (modified joystick) to across over an unknown obstacle to finally placed at the target. A brief discussion shows that the proposed method can realize life-long learning and endure more complex operational tasks.

## REFERENCES

[1]    H. Ravichandar, A. S. Polydoros, S. Chernova, and A. Billard, "Recent advances in robot learning from demonstration," *Annual Review of Control, Robotics, and Autonomous Systems*, vol. 3, pp. 297-330, 2020.

[2]    S. Schaal, "Dynamic movement primitives-a framework for motor control in humans and humanoid robotics," *Adaptive motion of animals and machines*, pp. 261-280: Springer, 2006.

[3]    M. Saveriano, F. J. Abu-Dakka, A. Kramberger, and L. Peternel, "Dynamic movement primitives in robotics: A tutorial survey," arXiv preprint arXiv:2102.03861, 2021.

[4]    Z. Li, T. Zhao, F. Chen, Y. Hu, C.-Y. Su, and T. Fukuda, "Reinforcement learning of manipulation and grasping using dynamical movement primitives for a humanoid like mobile manipulator," *IEEE/ASME Transactions on Mechatronics*, vol. 23, no. 1, pp. 121-131, 2017.

[5]    T. Zhao, M. Deng, Z. Li, and Y. Hu, "Cooperative manipulation for a mobile dual-arm robot using sequences of dynamic movement primitives," *IEEE Transactions on Cognitive and Developmental Systems*, vol. 12, no. 1, pp. 18-29, 2018.

[6]    D. H. Park, H. Hoffmann, P. Pastor, and S. Schaal, "Movement reproduction and obstacle avoidance with dynamic movement primitives and potential fields." in *Humanoids 2008-8th IEEE-RAS International Conference on Humanoid Robots*, Daejeon, Korea, 2008, pp. 91-98.

[7]    H. Tan, E. Erdemir, K. Kawamura, and Q. Du, "A potential field method-based extension of the dynamic movement primitive algorithm for imitation learning with obstacle avoidance." In *International Conference on Mechatronics and Automation*, Beijing, China, 2011, pp. 525-530.

[8]    H. Hoffmann, P. Pastor, D.-H. Park, and S. Schaal, "Biologically-inspired dynamical systems for movement generation: Automatic real-time goal adaptation and obstacle avoidance." In *IEEE International Conference on Robotics and Automation*, Kobe, Japan, 2009, pp. 2587-2592.

[9]    S. M. Khansari-Zadeh, and A. Billard, "A dynamical system approach to realtime obstacle avoidance," *Autonomous Robots*, vol. 32, no. 4, pp. 433-454, 2012.

[10]   A. Gams, T. Petrič, M. Do, B. Nemec, J. Morimoto, T. Asfour, and A. Ude, "Adaptation and coaching of periodic motion primitives through physical and visual interaction," *Robotics and Autonomous Systems*, vol. 75, pp. 340-351, 2016.

[11]   A. Rai, G. Sutanto, S. Schaal, and F. Meier, "Learning feedback terms for reactive planning and control." In *2017 IEEE International Conference on Robotics and Automation (ICRA)*, Singapore, 2017, pp. 2184-2191.

[12]   A.T. Khan, S. Li, and Z. Li, "Obstacle avoidance and model-free tracking control for home automation using bio-inspired approach." *Advanced*

[13]   Z. Lu, N. Wang, and C. Yang, "A Constrained DMP Framework for Robot Skills Learning and Generalization from Human Demonstrations," *IEEE/ASME Transactions on Mechatronics*, 2021. In press, DOI: 10.1109/TMECH. 2021.3057022

[14]   C. Yang, C. Zeng, C. Fang, W. He, and Z. Li, "A DMP-based framework for robot learning and generalization of humanlike variable impedance skills," *IEEE/ASME Transactions on Mechatronics*, vol. 23, no. 3, pp. 1193-1203, 2018.

[15]   C. Yang, C. Zeng, P. Liang, Z. Li, R. Li, and C.-Y. Su, "Interface design of a physical human–robot interaction system for human impedance adaptive skill transfer," *IEEE Transactions on Automation Science and Engineering*, vol. 15, no. 1, pp. 329-340, 2017.

[16]   A.T. Khan, S. Li, and X. Cao, "Control framework for cooperative robots in smart home using bio-inspired neural network." *Measurement*, vol. 167, p.108253. 2021.

[17]   A.T. Khan, S. Li, and X. Zhou, "Trajectory optimization of 5-link biped robot using beetle antennae search," *IEEE Transactions on Circuits and Systems II: Express Briefs*. 2021. DOI: 10.1109/TCSII.2021.3062639

[18]   D. Kulić, C. Ott, D. Lee, J. Ishikawa, and Y. Nakamura, "Incremental learning of full body motion primitives and their sequencing through human motion observation," *The International Journal of Robotics Research*, vol. 31, no.3, pp.330-345, 2012.

[19]   A. Lemme, R. F. Reinhart, and J. J. Steil, "Self-supervised bootstrapping of a movement primitive library from complex trajectories". in *IEEE-RAS International Conference on Humanoid Robots*, Madrid, Spain, 2014, pp. 726-732.

[20]   T. Matsubara, S.-H. Hyon, and J. Morimoto, "Learning stylistic dynamic movement primitives from multiple demonstrations." In *2010 IEEE/RSJ International Conference on Intelligent Robots and Systems*, pp. 1277-1283. IEEE, 2010.

[21]   T. Matsubara, S.-H. Hyon, and J. Morimoto, "Learning parametric dynamic movement primitives from multiple demonstrations," *Neural networks*, vol. 24, no. 5, pp. 493-500, 2011.

[22]   Y. Zhao, R. Xiong, L. Fang, and X. Dai, "Generating a style-adaptive trajectory from multiple demonstrations," *International Journal of Advanced Robotic Systems*, vol. 11, no. 7, pp. 103, 2014.

[23]   J. E. Young, T. Igarashi, E. Sharlin, D. Sakamoto, and J. Allen, "Design and evaluation techniques for authoring interactive and stylistic behaviors," *ACM Transactions on Interactive Intelligent Systems (TiiS)*, vol. 3, no. 4, pp. 1-36, 2014.

[24]   A. LaViers, and M. Egerstedt, "Style-based abstractions for human motion classification." In *2014 ACM/IEEE International Conference on Cyber-Physical Systems (ICCPS)*, Berlin, Germany, 2014, pp. 84-91.

[25]   R. Wang, Y. Wu, W. L. Chan, and K. P. Tee, "Dynamic movement primitives plus: For enhanced reproduction quality and efficient trajectory modification using truncated kernels and local biases." In *IEEE/RSJ International Conference on Intelligent Robots and Systems*, Daejeon, Korea, 2016, pp. 3765-3771.

[26]   Y. Wu, R. Wang, L. F. D'Haro, R. E. Banchs, and K. P. Tee, "Multi-modal robot apprenticeship: Imitation learning using linearly decayed DMP+ in a human-robot dialogue system." In *IEEE/RSJ International Conference on Intelligent Robots and Systems*, Madrid, Spain,2018, pp. 8582-8588.

[27]   M. Jin, S. H. Kang, and P. H. Chang, "Robust compliant motion control of robot with nonlinear friction using time-delay estimation," *IEEE Transactions on Industrial Electronics*, vol. 55, no. 1, pp. 258-269, 2008.

[28]   Z. Lu, P. Huang, and Z. Liu, "Predictive approach for sensorless bimanual teleoperation under random time delays with adaptive fuzzy control," *IEEE Transactions on Industrial Electronics*, vol. 65, no. 3, pp. 2439-2448, 2017.

[29]   Z. Liu, J. Zhou, and C. P. Chen, "Broad learning system: Feature extraction based on K-means clustering algorithm." In *4th International Conference on Information, Cybernetics and Computational Social Systems (ICCSS)*, Dalian, China 2017, pp. 683-687.

[30]   H. Huang, T. Zhang, C. Yang, and C. P. Chen, "Motor learning and generalization using broad learning adaptive neural control," *IEEE Transactions on Industrial Electronics*, vol. 67, no. 10, pp. 8608-8617, 2019.

[31]   H. Huang, C. Yang, and C. P. Chen, "Optimal robot-environment interaction under broad fuzzy neural adaptive control," *IEEE Transactions on Cybernetics*. Vol. 57, no. 7, pp. 3824-3835, 2021

[32]   C. Yang, Y. Jiang, J. Na, Z. Li, L. Cheng, and C.-Y. Su, "Finite-time convergence adaptive fuzzy control for dual-arm robot with unknown

kinematics and dynamics", *IEEE Transactions on Fuzzy Systems*, vol. 27, no. 3, 2019, pp. 574-588.

[33] Z. Li, C.-Y. Su, L. Wang, Z. Chen, and T. Chai, "Nonlinear disturbance observer-based control design for a robotic exoskeleton incorporating fuzzy approximation," *IEEE Transactions on Industrial Electronics*, vol. 62, no. 9, pp. 5763-5775, 2015.

[34] C. Chen, J. Huang, D. Wu, and X. Tu, "Interval Type-2 Fuzzy disturbance observer-based TS fuzzy control for a pneumatic flexible joint," *IEEE Transactions on Industrial Electronics*. In press. 2021.

[35] J. Huang, M. Ri, D. Wu, and S. Ri, "Interval type-2 fuzzy logic modeling and control of a mobile two-wheeled inverted pendulum," *IEEE Transactions on Fuzzy Systems*, vol. 26, no. 4, pp. 2030-2038, 2017.

[36] J. Huang, W. Huo, W. Xu, S. Mohammed, and Y. Amirat, "Control of upper-limb power-assist exoskeleton using a human-robot interface based on motion intention recognition," *IEEE transactions on automation science and engineering*, vol. 12, no. 4, pp. 1257-1270, 2015.

[37] K. Xing, P. Yang, J. Huang, Y. Wang, and Q. Zhu, "A real-time EMG pattern recognition method for virtual myoelectric hand control," *Neurocomputing*, vol. 136, pp. 345-355, 2014.

[38] Y. Hu, X. Wu, P. Geng, and Z. Li, "Evolution strategies learning with variable impedance control for grasping under uncertainty," *IEEE Transactions on Industrial Electronics*, vol. 66, no. 10, pp. 7788-7799, 2018.

[39] C. Yang, G. Peng, Y. Li, R. Cui, L. Cheng, and Z. Li, "Neural networks enhanced adaptive admittance control of optimized robot–environment interaction,*" IEEE transactions on cybernetics*, vol. 49, no. 7, pp. 2568-2579, 2018.

[40] C. Yang, G. Peng, L. Cheng, J. Na, and Z. Li, "Force Sensorless Admittance Control for Teleoperation of Uncertain Robot Manipulator using Neural Networks", *IEEE Transactions on Systems, Man, and Cybernetics: Systems,* vol. 51, no. 5, pp. 3282-3292, 2021.

[41] T. Sansanayuth, I. Nilkhamhang, and K. Tungpimolrat, "Teleoperation with inverse dynamics control for phantom omni haptic device, " In *2012 Proceedings of SICE Annual Conference (SICE)*, Akita, Japan, 2012, pp. 2121-2126.